Dynamic Buckling of Imperfection-Sensitive Shell Structures

Sunil Saigal*
Worcester Polytechnic Institute, Worcester, Massachusetts
T. Y. Yang†
Purdue University, West Lafayette, Indiana
and
Rakesh K. Kapania‡
Virginia Polytechnic Institute and State University, Blacksburg, Virginia

Structural buckling under dynamic loads may occur at load levels that are less than the corresponding static loads. Presence of local geometric imperfections may induce an early buckling for both static and dynamic loadings. The phenomenon of "dynamic weakening" is studied for a general class of shell structures under a general class of time-dependent loadings. A doubly curved quadrilateral Love-Kirchhoff shell finite element is used. Geometric deviations of the shell middle surface are included within the element formulation by suitably modifying the strain-displacement relations. This is accomplished by retaining additional terms that are quadratic in spatial derivatives of imperfections and displacement components. The nonlinear equations of motion are written in the Lagrangian system and are solved by using an incremental algorithm based on Newmark's generalized operator. The dynamic responses up to buckling are obtained for a perfect spherical cap and an imperfect spherical cap both under external pressure, as well as a complete imperfect sphere under external pressure. Numerical results include the effects of amplitude of imperfection and thickness of shell on the dynamic buckling loads. The formulation is general and can be applied to obtain the dynamic buckling responses of a wide variety of shell structures.

Introduction

DYNAMIC buckling is defined as the threshold load at which large increases in peak amplitude of the average dynamic displacement occur. It is an important cause of structural failure and has constituted a major field of research in structural mechanics.

The study of dynamic buckling of shells has largely been conducted for the case of spherical caps. The dynamic snap-through of clamped spherical caps was analyzed by Humphrey and Bodner[1] for impulsive loading and by Budiansky and Roth[2] and Simitses[3] for step loading using the Rayleigh-Ritz method. Archer and Lange[4] used a numerical technique based on the finite-difference method. Other numerical solutions of this problem were given by Huang,[5] Stephens and Fulton,[6] Stricklin and Martinez,[7] Stricklin et al.,[8] and Ball and Burt.[9] Experimental results were obtained by Lock et al.[10] All of these studies were done for the case of axisymmetric snap-through behavior. The asymmetric behavior has received some attention, and the perturbation approach was utilized to treat the asymmetric deformation mode.[8,11]

The effect of initial imperfections on static shell buckling analysis has received much attention, and some of the later reviews of these efforts are by Bushnell,[12] Babcock,[13] and Kapania and Yang.[14] The dynamic buckling of an externally pressurized imperfect sphere was presented by McNamara and Marcal.[15] Dynamic buckling curves for imperfect spherical caps clamped at the ends were given by Kao and Perrone,[16] and a perturbation analysis for imperfect cylindrical shells was given by Lockhart.[17] Review papers on the subject of dynamic buckling of shells were given by Holzer[18] and Jones.[19]

In this paper, a finite-element analysis of the dynamic buckling response of a general class of shells with arbitrary prescribed geometric imperfections is presented. A 48-degree-of-freedom (dof) doubly curved quadrilateral Love-Kirchhoff shell finite element whose formulations include the effect of geometric imperfections is used. Both the geometry and the imperfections are defined using variable-order polynomials, allowing a wide variety of shells with general imperfections to be treated. The developments are not limited to analysis of restricted geometries, e.g., axisymmetric, or special imperfections, e.g., sinusoidal.

To account accurately for rigid-body modes, the Cartesian displacement components are used to express the shell displacements. The capability to accurately include the rigid-body modes is essential if the element has to be used for problems that entail large displacements.[20] The present element is an extended version of the element formulated by Moore et al.[21] and Yang and Saigal[22] to study the linear and geometrically nonlinear behavior of perfect shells of arbitrary shape.

The strain-displacement relations for imperfect shells are represented in terms of Cartesian displacement components and are an extended version of the strain-displacement relations given in tensorial form by Niordson[23] for perfect shells. The nonlinear effects are included using an incremental formulation based on the Lagrangian mode of description of motion. The resulting equations are linearized and solved by using a numerical integration procedure based on Newmark's generalized operator. Adequate validation of the present developments is done by a detailed study of dynamic buckling responses of a clamped spherical cap under external pressure

Presented as Paper 86-0966 at the AIAA/ASME/ASCE/AHS 27th Structures, Structural Dynamics and Materials Conference, San Antonio, TX, May 19–21, 1986; received June 10, 1986; revision received Feb. 17, 1987.

*Assistant Professor, Mechanical Engineering Department. Associate Member AIAA.

†Professor of Aeronautics and Astronautics, Dean of Engineering, School of Aeronautics and Astronautics. Fellow AIAA.

‡Assistant Professor, Department of Aerospace and Ocean Engineering. Member AIAA.

and a complete sphere under external pressure. Results are obtained for various imperfection amplitudes and thicknesses of the shells with good agreement with existing alternative solutions. An important contribution of the present study is the inclusion of geometric imperfection within an element formulation in a finite-element displacement model. This precludes the difficulties encountered in ensuring continuity of displacements across element junctions when imperfections are modeled by suitably arranging elements in finite-element discretization[15] of the structure.

Shell Finite Element

Strain-Displacement Relations

The shape of the shell is defined by the middle surface of the shell and the thickness h. The middle surface, which is smooth but otherwise of arbitrary shape, is defined by a vector $\boldsymbol{r}$, which is given as

$$\boldsymbol{r} = x^i \boldsymbol{e}_i; \quad i = 1,2,3 \tag{1}$$

where x^i is a fixed Cartesian coordinate system in three-dimensional space in which the middle surface is embedded, and $\boldsymbol{e}_i$ is a unit vector in the x^i direction.

The middle surface is also described by means of a system of parametric relations

$$x^i = f^i(\theta^1, \theta^2) \tag{2}$$

in which the parameters θ^α ($\alpha = 1,2$) serve as coordinates on the surface and can be regarded as being an arbitrarily selected system. The two base vectors $\boldsymbol{a}_1$ and $\boldsymbol{a}_2$ are obtained as derivatives of $\boldsymbol{r}$ with respect to each component θ^α and are denoted by $\boldsymbol{a}_\alpha$, i.e.,

$$\boldsymbol{a}_\alpha = \boldsymbol{r},_\alpha = \frac{\partial f^i}{\partial \theta^\alpha} \boldsymbol{e}_i = f^i_{,\alpha} \boldsymbol{e}_i \tag{3}$$

The unit normal to the surface $\boldsymbol{a}_3$ is given as

$$\boldsymbol{a}_3 = \frac{\boldsymbol{a}_1 \times \boldsymbol{a}_2}{|\boldsymbol{a}_1 \times \boldsymbol{a}_2|} = n^i \boldsymbol{e}_i \tag{4}$$

where

$$n^i = c e_{ijk} f^j_{,1} f^k_{,2} \tag{5}$$

e_{ijk} is the alternating symbol, and

$$c = [|\boldsymbol{a}_1 \times \boldsymbol{a}_2|]^{-1} = 1/\sqrt{\boldsymbol{a}} \tag{6}$$

and

$$a = \begin{vmatrix} a_{11} & a_{12} \\ a_{21} & a_{22} \end{vmatrix} \tag{7}$$

where

$$a_{\alpha\beta} = \boldsymbol{a}_\alpha \boldsymbol{a}_\beta = f^i_{,\alpha} f^i_{,\beta} \tag{8}$$

$a_{\alpha\beta}$ is the metric tensor, and it yields the first fundamental form of a surface

$$ds^2 = a_{\alpha\beta}\, \mathrm{d}\theta^\alpha\, \mathrm{d}\theta^\beta \tag{9}$$

where ds is the distance between two neighboring points at θ^α and $\theta^\alpha + \mathrm{d}\theta^\alpha$ ($\alpha = 1,2$). Similarly, the second fundamental tensor or the curvature tensor of the surface, $b_{\alpha\beta}$, is given as

$$b_{\alpha\beta} = n^i \frac{\partial^2 f^i}{\partial\theta^\alpha \partial\theta^\beta} = n^i f^i_{,\alpha\beta} \tag{10}$$

A point on the middle surface with the coordinates θ^α has the Cartesian coordinates $f^i(\theta^1, \theta^2)$ in the initial state. After deformation, the same point has the Cartesian coordinates $f^i + u^i$, where u^i are the Cartesian components of the displacement vector, and give complete information about the deformation of the middle surface.

In the deformed state, the fundamental and the curvature tensors take the form $\bar{a}_{\alpha\beta}$ and $\bar{b}_{\alpha\beta}$, respectively.

$$\bar{a}_{\alpha\beta} = (f^i + u^i)_{,\alpha} (f^i + u^i)_{,\beta} = \bar{f}^i_{,\alpha} \bar{f}^i_{,\beta} \tag{11}$$

$$\bar{b}_{\alpha\beta} = \bar{n}^i \bar{f}^i_{,\alpha\beta} \tag{12}$$

where

$$\bar{n}^i = (\bar{a})^{-\frac{1}{2}} e_{ijk} \bar{f}^j_{,1} \bar{f}^k_{,2} \tag{13}$$

The value of $(\bar{a})^{-\frac{1}{2}}$ can be approximated as

$$(\bar{a})^{-\frac{1}{2}} = (a)^{-\frac{1}{2}}[1 - (A/a)]$$

where

$$A = (\varepsilon_{11} a_{22} + \varepsilon_{22} a_{11} - 2\varepsilon_{11} a_{12}) \tag{14}$$

In Eq. (14), $\varepsilon_{\alpha\beta}$ are the tangential strain measures, and are given as

$$\varepsilon_{\alpha\beta} = \tfrac{1}{2}(\bar{a}_{\alpha\beta} - a_{\alpha\beta}) = \tfrac{1}{2}(f^i_{,\alpha} u^i_{,\beta} + u^i_{,\alpha} f^i_{,\beta} + u^i_{,\alpha} u^i_{,\beta}); \quad i = 1,2,3 \tag{15}$$

The terms $u^i_{,\alpha}$ and $u^i_{,\beta}$ are the nonlinear terms that are neglected in linear analysis but are retained in the present study.

The curvature measure is given as

$$k_{\alpha\beta} = -(\bar{b}_{\alpha\beta} - b_{\alpha\beta}) + \tfrac{1}{2}(b^\delta_\alpha \varepsilon_{\beta\delta} + b^\delta_\beta \varepsilon_{\alpha\delta}) \tag{16}$$

The final expression for $k_{\alpha\beta}$ is obtained by substitution of relations given in Eqs. (12–14) into Eq. (16) and neglecting the nonlinear terms in the derivation of curvature.

Imperfect Shells

For the case of an imperfect shell, let v^i be the Cartesian components of the imperfection at a given point on the shell surface. The Cartesian coordinates of the given point in an undeformed configuration then become $(f^i + v^i)$, and after deformation the same point will have the Cartesian coordinates as $(f^i + v^i + u^i)$. The tangential strain measures then become

$$\begin{aligned} \varepsilon_{\alpha\beta} &= \tfrac{1}{2}[(f^i + v^i + u^i)_{,\alpha}(f^i + v^i + u^i)_{,\beta} - (f^i + v^i)_{,\alpha}(f^i + v^i)_{,\beta}] \\ &= \tfrac{1}{2}(f^i_{,\alpha} u^i_{,\beta} + f^i_{,\beta} u^i_{,\alpha} + u^i_{,\alpha} u^i_{,\beta} + v^i_{,\alpha} u^i_{,\beta} + v^i_{,\beta} u^i_{,\alpha}) \end{aligned} \tag{17}$$

In this study, the effects of imperfections on the curvature-displacement relationships are ignored. This assumption is the same as that made by Koiter.[24]

Element Geometry and Imperfections

The thin-shell finite element is quadrilateral in shape and has four corner nodal points. The middle surface of the shell finite element is assumed to be described by a polynomial function. The Cartesian coordinates x^1, x^2, and x^3 and the imperfections v^1, v^2, and v^3 of the middle surface of the shell finite element can be described by polynomial functions of the curvilinear coordinates ξ and η with a total of N terms.

$$x^i(\xi,\eta) = \sum_{j=1}^{N} c^i_j \xi^{m_j} \eta^{n_j} \tag{18}$$

$$v^i(\xi,\eta) = \sum_{j=1}^{N} \bar{c}^i_j \xi^{m_j} \eta^{n_j}, \quad i = 1,2,3 \tag{19}$$

where the constants m_j and n_j define the power of ξ and η, respectively, for the jth term. The constants c^i_j and $\bar{c}^i_j$ are solved based on the coordinates x^i and imperfections v^i ($i = 1,2,3$) at

N selected points on the middle surface of the shell element. If the points are equidistant from each other, one can use the Lagrangian interpolation polynomials. Similarly, one can also employ B-spline and rational B-spline polynomials to represent the shell surface and the imperfections.

Strain Energy and Element Matrices Formulations

The functional of the total potential energy can be written as

$$J_p(u) = \iint_A \{W[\varepsilon_{\alpha\beta}(u),k_{\alpha\beta}(u)] - p^i u^i\} \sqrt{a}\, \mathrm{d}\theta^1 \mathrm{d}\theta^2 \tag{20}$$

where W is the strain energy density per unit undeformed middle surface of the shell, and is given as

$$W = \frac{1}{2} H^{\alpha\beta\lambda\mu}\left(\varepsilon_{\alpha\beta}\varepsilon_{\lambda\mu} + \frac{h^2}{12} k_{\alpha\beta}\, k_{\lambda\mu}\right) \tag{21}$$

with the tensor of elastic moduli

$$H^{\alpha\beta\lambda\delta} = \frac{Eh}{2(1+v)}\left[a^{\alpha\lambda}a^{\beta\mu} + a^{\alpha\mu}a^{\beta\lambda} + \frac{2v}{1-v} a^{\alpha\beta}a^{\lambda\mu}\right] \tag{22}$$

In Eq. (22), E is Young's modulus and v is Poisson's ratio, $a^{\alpha\beta}$ are the contravariant components of the metric tensor and are related to $a_{\alpha\beta}$ through the relation

$$a^{\alpha\lambda}a_{\lambda\beta} = \delta^{\alpha}_{\beta} \tag{23}$$

where δ^{α}_{β} is the Kronecker symbol. The p^i are the Cartesian components of the applied pressure in three directions.

It is noted that the constitutive equations are defined by the partial derivatives of $W(\varepsilon_{\alpha\beta},k_{\alpha\beta})$ with respect to the strain measures $\varepsilon^{\alpha\beta}$ and $k_{\alpha\beta}$.

$$\begin{aligned} \frac{\partial W}{\partial \varepsilon_{\alpha\beta}} &= N^{\alpha\beta} = H^{\alpha\beta\lambda\mu}\, \varepsilon_{\lambda\mu} \\ \frac{\partial W}{\partial k_{\alpha\beta}} &= M^{\alpha\beta} = \frac{h^2}{12} H^{\alpha\beta\lambda\mu}\, k_{\lambda\mu} \end{aligned} \tag{24}$$

Here $N^{\alpha\beta}$ is the stress resultant tensor and $M^{\alpha\beta}$ is the stress couple tensor. In this study, the incremental solution procedure was used. Only a brief description of the derivation of the tangent stiffness matrix is given. A detailed description of the derivation of the incremental equations of motion can be found in Refs. 25 and 26. Since total Lagrangian formulation is used, all field quantities of shell deformations are referred to the known undeformed shell middle surface. Let $\bar{u}$ be the displacement vector of a material point in the undeformed shell middle surface to its position in the deformed configuration. Let $\hat{u}$ be the incremental displacement vector of the same point.

Referred to the undeformed middle surface, the displacement field of the final configuration can be expressed as

$$\underline{u} = \underline{\bar{u}} + \underline{\hat{u}} \tag{25}$$

The middle surface strain tensor $\varepsilon_{\alpha\beta}$ and the curvature tensor are given as

$$\varepsilon_{\alpha\beta} = \bar{\varepsilon}_{\alpha\beta} + \hat{\varepsilon}_{\alpha\beta} \tag{26}$$

$$k_{\alpha\beta} = \bar{k}_{\alpha\beta} + \hat{k}_{\alpha\beta} \tag{27}$$

where $\bar{\varepsilon}_{\alpha\beta}$ is obtained by substituting $\bar{u}$ in Eq. (17). Similarly, $\bar{k}_{\alpha\beta}$ and $\hat{k}_{\alpha\beta}$ can be obtained by substituting $\bar{u}$ and $\hat{u}$, respectively, in Eq. (16) after using Eqs. (12–14).

Because of the presence of nonlinear terms in Eq. (17), $\hat{\varepsilon}_{\alpha\beta}$ cannot be obtained by merely substituting $\hat{u}$ in Eq. (17). It is a function of both $\bar{u}$ and $\hat{u}$.

It can be seen that the incremental strain tensor is given as

$$\begin{aligned} \hat{\varepsilon}_{\alpha\beta} &= \varepsilon_{\alpha\beta}(\underline{u}) - \varepsilon_{\alpha\beta}(\underline{\bar{u}}) \\ &= \tfrac{1}{2}(f^i_{,\alpha}\, \hat{u}^i_{,\beta} + f^i_{,\beta}\, \hat{u}^i_{,\alpha} + \hat{u}^i_{,\alpha}\, \hat{u}^i_{,\beta} + \bar{u}^i_{,\alpha}\, u^i_{,\beta} \\ &\quad + \bar{u}^i_{,\beta}\, \hat{u}^i_{,\alpha} + v^i_{,\alpha}\, \hat{u}^i_{,\beta} + v^i_{,\beta}\, \hat{u}^i_{,\alpha}) \end{aligned} \tag{28}$$

From Eqs. (16) and (28), we can write the expression for incremental strain and curvatures as

$$\{\mathrm{d}\varepsilon\} = \begin{Bmatrix} \hat{\varepsilon}_{\alpha\beta} \\ \hat{k}_{\alpha\beta} \end{Bmatrix} = [A_0 + A_i + A_L(\underline{\bar{u}})]\{\underline{\hat{u}}\} \tag{29}$$

where A_0 is the same matrix as in linear infinitesimal strain analysis, A_i the matrix due to imperfections, and A_L depends upon the displacements $\{\bar{u}\}$.

The three components of the incremental displacement vector are related to the element degrees of freedom $\{\hat{q}_e\}$ through the element shape functions $[N]$

$$\{\underline{\hat{u}}\} = [N]\{\hat{q}_e\} \tag{30}$$

Substituting Eq. (30) in Eq. (29), we get

$$\{\mathrm{d}\varepsilon\} = [B_0 + B_i + B_L(q_e)]\{\hat{q}_e\} \tag{31}$$

The tangent stiffness matrix is given as

$$\begin{aligned} [k_T] = &\iint_A [B_0 + B_i + B_L(q_e)]^T [D] \\ &[B_0 + B_i + B_L(q_e)]\sqrt{a}\, \mathrm{d}\theta^1\, \mathrm{d}\theta^2 + \iint_A [G]^T[H][G]\sqrt{a}\, \mathrm{d}\theta^1\, \mathrm{d}\theta^2 \end{aligned} \tag{32}$$

In Eq. (32), $[D]$ is the 6×6 stress-strain matrix as given by Eq. (24). The second integral yields the well-known incremental stiffness matrix. The matrix $[G]$ is given as

$$[\hat{u}^1_{,1}\ \hat{u}^2_{,1}\ \hat{u}^3_{,1}\ \hat{u}^1_{,2}\ \hat{u}^2_{,2}\ \hat{u}^3_{,2}]^T = [G]\{\hat{q}_e\} \tag{33}$$

The matrix $[H]$ is given as

$$[H] = \begin{bmatrix} H_{11} & H_{12} \\ H_{21} & H_{22} \end{bmatrix}; \quad H_{\alpha\beta} = N^{\alpha\beta}\begin{bmatrix} 1 & 0 & 0 \\ 0 & 1 & 0 \\ 0 & 0 & 1 \end{bmatrix} \tag{34}$$

The incremental load vector $\{\hat{p}_e\}$ is given as

$$\{\hat{p}_e\} = \{p_e\} - \iint_A [B_0 + B_i + B_L(q)]^T \begin{Bmatrix} N^{\alpha\beta}(q) \\ M^{\alpha\beta}(q) \end{Bmatrix} \sqrt{a}\, \mathrm{d}\theta^1\, \mathrm{d}\theta^2 \tag{35}$$

where $\{p_e\}$ is the total applied load vector and the second term yields the total internal load vector.

The formulations of matrices in this section were checked by performing the limit load analysis for a complete spherical shell with modal imperfections of wave number 16 given by

$$a = -a_0 h\, P_{16}(\cos\phi)$$

where P_{16} is the Legendre polynomial of order 16 and ϕ is the angle between the pole and a point on the meridian of the perfect sphere. The imperfection-sensitivity as a function of the imperfection wave number was discussed by Hui and Leissa.[27] The geometric and material data for the sphere are shown in Fig. 1. Due to axisymmetry, a 10-deg segment of the upper half of the sphere was modeled using nine equal elements. Figure 1

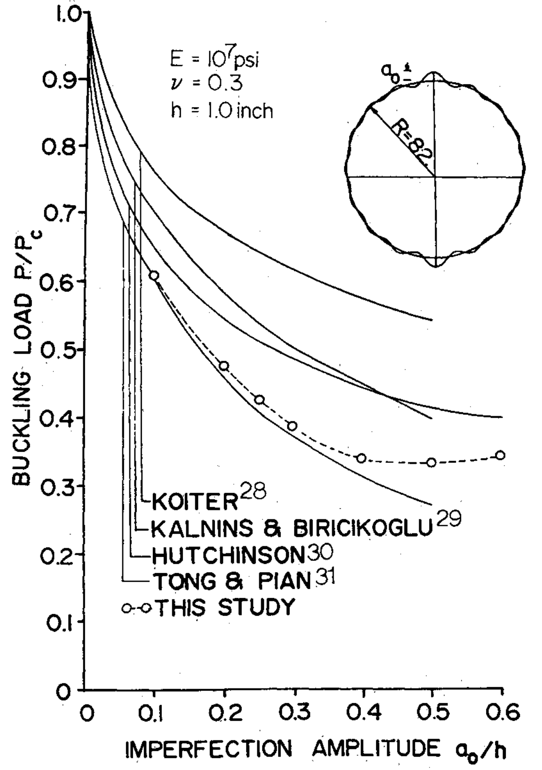

Fig. 1 Imperfection-sensitivity of a pressure-loaded complete spherical shell.

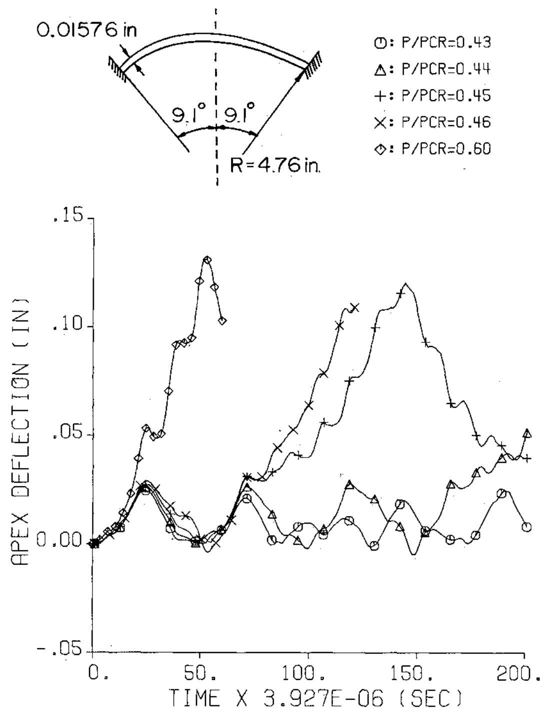

Fig. 2 Dynamic responses up to buckling of a clamped, geometrically perfect, spherical cap under step uniform external pressure.

shows the nondimensional limit buckling pressure $P_c\,[=2E(h/R)^2/\sqrt{3(1-\nu^2)}]$ for different values of a_0. For comparison, some alternative solutions were also shown: by Koiter[28] using the initial postbuckling analysis, by Kalnins and Biricikoglu,[29] by Hutchinson,[30] and by Tong and Pian.[31] The present results are closer to those obtained by Tong and Pian[31] in the region of $a_0 < 0.4$.

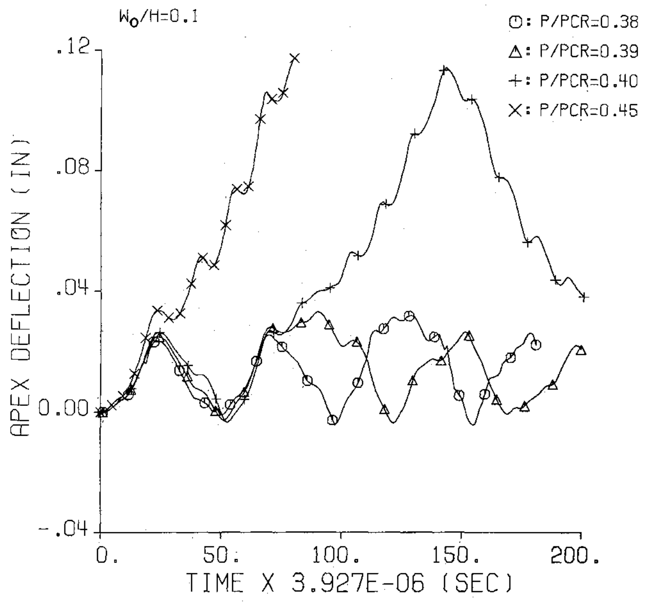

Fig. 3 Dynamic responses up to buckling of a clamped, imperfect ($W_0 = 0.1$) spherical cap under step uniform external pressure.

Nonlinear Dynamics and Solution Procedures

The linearized incremental equations of motion for an assemblage of nonlinear finite elements are given as[25]

$$[M]\{\ddot{Q}(t+\Delta t)\} + [C]\{\dot{Q}(t+\Delta t)\} + [K_T(t)]\{\Delta Q\} = \{F\{t+\Delta t)\} - \{R(t)\} \tag{36}$$

where $[M]$ and $[C]$ are the mass and damping matrices, respectively; $[K_T(t)]$ the tangent stiffness matrix at time t; $\{Q(t+\Delta t)\}$, $\{\dot{Q}(t+\Delta t)\}$, and $\{\ddot{Q}(t+\Delta t)\}$ the vectors of nodal displacements, velocities, and accelerations at time $t+\Delta t$, respectively; $\{\Delta Q\} = \{Q(t+\Delta t)\} - \{Q(t)\}$ the vector of displacement increment; $\{F(t+\Delta t)\}$ the vector of applied loads at time $t+\Delta t$; and $\{R(t)\}$ the vector of nodal forces corresponding to element stresses at time t.

The solution of Eq. (36) yields only approximate displacement increments $\{\Delta Q\}$. To improve the solution accuracy and, in some cases, to prevent the solution instabilities, iterations to achieve equilibrium at the end of each or some preselected time steps may be performed. For an iterative step i, the equilibrium equations are expressed as

$$[M]\{\ddot{Q}(t+\Delta t)\}^i + [C]\{\dot{Q}(t+\Delta t)\}^i + [K_T(t)]\{\Delta Q\}^i = \{F(t+\Delta t)\} - \{R(t+\Delta t)\}^{i-1} \tag{37}$$

where $\{\ddot{Q}(t+\Delta t)\}^i$ and $\{\dot{Q}(t+\Delta t)\}^i$ are the approximations to the accelerations and velocities, respectively, obtained in iteration i and depend on the numerical time integration scheme used. The vector of nodal point forces $\{R(t+\Delta t)\}^{i-1}$ is determined from the element stresses in the configuration corresponding to displacements $\{Q(t+\Delta t)\}^{i-1}$. Consistent formulations were used in this study to determine the mass matrix.

In the present study, Newmark's scheme for numerical integration is used to determine the nonlinear responses. For each time step, modified Newton-Raphson iterations are applied to achieve equilibrium at the end of that step. A detailed algorithm for this scheme can be found in, for example, Ref. 25.

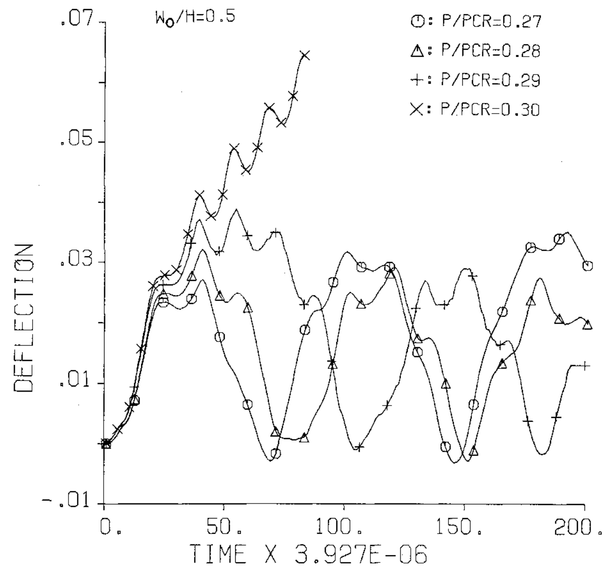

Fig. 4 Dynamic responses up to buckling of a clamped, imperfect ($W_0 = 0.5$) spherical cap under step uniform external pressure.

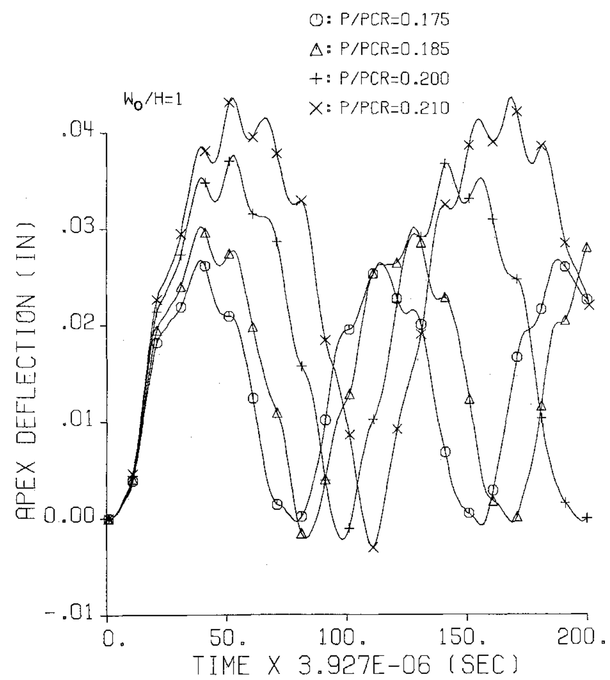

Fig. 5 Dynamic responses up to buckling a clamped, imperfect ($W_0 = 1.0$) spherical cap under step uniform external pressure.

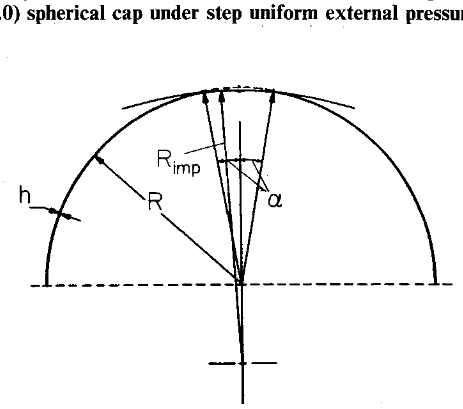

Fig. 6 Hemisphere of externally pressurized imperfect complete sphere. $R = 0.812$ in., $\alpha = 10$ deg, $R/R_{imp} = 1.15$, $E = 10.6 \times 10^6$ psi, $\nu = 0.274$.

The iterations for every incremental time step were terminated when the following convergence criterion was satisfied:

$$\left(\sum_{i=1}^{N} (\Delta Q_i^r)^2 \Big/ \sum_{i=1}^{N} (Q_i^r)^2 \right)^{\frac{1}{2}} \leq 0.01\%$$

where the subscript i is the dof number and N is the total number of dof's of the finite-element modeling, the superscript r is the iterative cycle number, ΔQ is the displacement increment, and Q is the accumulated displacement.

Numerical Results

The dynamic response up to buckling of a spherical cap and a complete sphere were obtained using the present formulations. Qualitatively, if the time histories of the modes of deformation are given for several levels of a constantly applied load, the critical buckling load can simply be identified as the load at which a large increase in the amplitudes of the deformations is seen to occur.[32] Following such a procedure, the time histories of peak responses of various shells were obtained to determine the state of dynamic buckling. Descriptions of dynamic buckling criterion are given in, for example, Refs. 16 and 32.

All results presented in this paper were obtained using a CYBER 205 supercomputer at Purdue University.

Spherical Cap Without Imperfections

A clamped spherical cap, shown in Fig. 2, under step external pressure and without initial geometric imperfections was first studied. The nondimensional quantities for this cap are: $q = P/P_{cr}$, $P_{cr} = 4Eh^2/R^2m^2$, $m^4 = 12(1-\nu^2)$, where P is the applied external pressure, E the modulus of elasticity, ν Poisson's ratio, h the thickness, and R the radius of the cap.

Due to axisymmetry, six elements were used to model a 10-deg sector of the cap. A time step $\Delta t = 3.927$ μs was used to obtain the time histories for the first 785 μs of response. The response histories obtained for the apex displacement are plotted in Fig. 2. Increasing amplitudes of peak response were observed for $P/P_{cr} = 0.44$ after 600 μs. A value of $P/P_{cr} = 0.46$ was reported as the dynamic buckling estimate of this cap by Kao and Perrone[16] based on interpolation of average displacement measure. Their analysis was based on a finite-difference mesh and a nonlinear relaxation method for solution of resulting nonlinear equations. A good agreement in trends and the value of the critical load is seen.

Spherical Cap with Imperfections

The spherical cap described in the previous section was next analyzed with initial geometric dimple-type imperfections given in the form

$$w_i = (W_0/h)(1-x^2)^3$$

where W_0 is the maximum imperfection that occurs at the shell apex, $x = r/R$, and r is the radial distance of a point on the cap from the axis of the cap. Such imperfection was also used by Koga and Hoff.[33] The same finite-element model and time step as for the perfect spherical cap were used. The time responses were obtained for the first 785 μs for the three cases when $W_0 = 0.1$, 0.5, and 1.0. The time histories of apex displacement for increasing level of external pressure on the cap were shown in Figs. 3–5 for the three cases, respectively. Sudden jumps in the amplitude of peak displacement near the critical load were obvious for the cases when $W_0 = 0.1$ and 0.5. Such a drastic change, however, was not seen for $W_0 = 1.0$. This trend was also observed by Kao and Perrone[16] using their finite-difference scheme. The nondimensional buckling pressures obtained in the present study based on the first 785 μs of response histories were within 7% of those obtained by Kao and Perrone.[16] Closer agreement may have been obtained by studies based on longer time histories. The present formulations, however, exhibit a good agreement in trends. This investigation confirms that initial imperfections do have the effect of reducing dynamic buckling capacity of spherical caps.

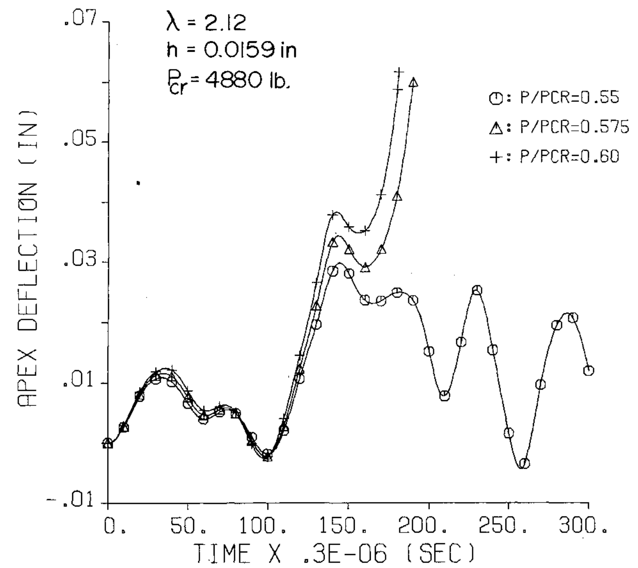

Fig. 7 Dynamic responses up to buckling of imperfect complete spherical shell ($\lambda = 2.12$) under step internal pressure.

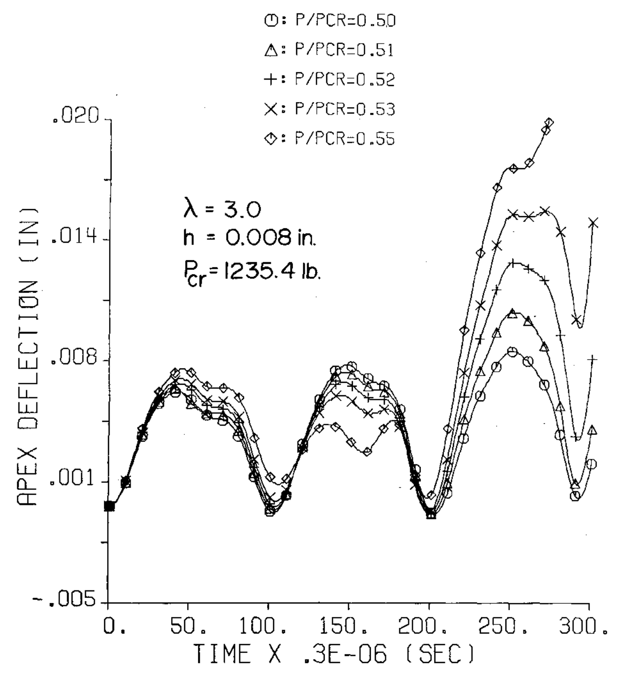

Fig. 8 Dynamic responses up to buckling of imperfect complete spherical shell ($\lambda = 3.0$) under step internal pressure.

Complete Sphere with Imperfections

The geometry of the sphere is shown in Fig. 6, where the imperfection is given as a flat section of the shell of radius R_{imp}, which is taken to be the mean radius of the oblate portion of the sphere. The geometric parameter for the shell is defined as $\lambda = 12(1-\nu^2)^{1/4}\ (R/h)^{1/2}(R/R_{imp})^{1/2}\alpha$. This problem was previously studied by McNamara and Marcal[15] using high-order isoparametric elements. The geometric imperfection was accounted for by using separate discretization of the imperfect portion and by applying a constraint relating the displacements at two hypothetical nodes[34] to assure continuity across the junction. Using such an approach requires special considerations for different types of imperfections and special solution algorithms may also be needed. The present developments, however, include initial geometric imperfections within the element formulations and do not require any special considerations.

A 10-deg segment of the half-sphere was modeled using nine elements due to axisymmetry. Four of these nine elements were used in the region of geometric imperfection to accurately model the imperfection. A time step of 0.3 μs was used for numerical integration as compared to the time step of 0.1 μs used in Ref. 15. The time responses of apex displacement are plotted in Fig. 7 for increasing values of external pressure. These time responses are the same as those obtained by McNamara and Marcal[15] for the same values of external pressure (and thus the results of Ref. 15 were not plotted in Fig. 7). Divergence between the deflection profiles for $P/P_{cr} = 0.575$ and 0.55, where $P_{cr} = 2E(t/R)^2/[3(1-\nu^2)]^{1/2}$ as observed in Ref. 15, is also seen here.

The same sphere was also analyzed by reducing the thickness of the shell. The number of elements and size of time step for numerical integration used were the same as in the previous analysis. The time responses of apex displacements for this case were shown in Fig. 8. A reduction in the value of critical internal pressure for dynamic buckling was seen.

Concluding Remarks

A nonlinear analysis has been presented for estimating the dynamic buckling behavior of thin-shell structures with arbitrary geometric imperfections and arbitrary loadings. The treatment of initial geometric deviations has been included within the element formulations, thus avoiding the need for special techniques to treat displacement continuity requirements at the junction of imperfect portion with the rest of the shell.[15] Numerical studies have been presented to indicate the effects of geometric imperfection and shell thickness on the dynamic response and the critical load for dynamic buckling. The present examples also indicate, as pointed out by previous workers, that the critical load decreases with increases in amplitude of imperfection and with decreases in shell thicknesses. The present formulation and analysis method may provide an effective tool for the nonlinear study of dynamic buckling of general imperfect thin elastic shells.

References

[1]Humphrey, J. S. and Bodner, S. R., "Dynamic Buckling of Shallow Shells Under Impulsive Loading," *Journal of the Engineering Mechanics Division, Proceedings of the ASCE*, Vol. 88, 1962, pp. 17–35.

[2]Budiansky, B. and Roth, R. S., "Axisymmetric Dynamic Buckling of Clamped Shallow Spherical Shells," NASA TND-1510, 1962, pp. 597–606.

[3]Simitses, G. J., "Axisymmetric Dynamic Snap-Through Buckling of Shallow Spherical Shells," *AIAA Journal*, Vol. 5, 1967, pp. 1019–1021.

[4]Archer, R. R. and Lange, C. G., "Nonlinear Dynamic Behavior of Shallow Spherical Shells," *AIAA Journal*, Vol. 3, 1965, pp. 2313–2317.

[5]Huang, N. C., "Axisymmetric Dynamic Snap-Through of Elastic Clamped Shallow Spherical Shells," *AIAA Journal*, Vol. 7, 1969, pp. 215–220.

[6]Stephens, W. B. and Fulton, R. E., "Axisymmetric Static and Dynamic Buckling of Spherical Caps Due to Centrally Distributed Pressures," *AIAA Journal*, Vol. 7, 1969, pp. 2120–2126.

[7]Stricklin, J. A. and Martinez, J. E., "Dynamic Buckling of Clamped Spherical Caps Under Step Pressure Loadings," *AIAA Journal*, Vol. 7, 1969, pp. 1212–1213.

[8]Stricklin, J. A., Martinez, J. E., Tillerson, J. R., Hong, J. H., and Haisler, W. E., "Nonlinear Dynamic Analysis of Shells of Revolution by Matrix Displacement Method," *AIAA Journal*, Vol. 9, 1971, pp. 629–636.

[9]Ball, R. E. and Burt, J. A., "Dynamic Buckling of Shallow Spherical Shells," *Journal of Applied Mechanics, Proceedings of the ASME*, June 1973, pp. 411–416.

[10]Lock, M. H., Okubo, S., and Whittier, J. S., "Experiments on the Snapping of a Shallow Dome Under a Step Pressure Load," *AIAA Journal*, Vol. 6, 1968, pp. 1320–1326.

[11]Akkas, N., "Bifurcation and Snap-through Phenomena in Axisymmetric Dynamic Analysis of Shallow Spherical Shells," *Computers and Structures*, Vol. 6, 1976, pp. 241–251.

[12]Bushnell, D., "Computerized Buckling Analysis of Shells," AFWAL-TR-81-3049, Dec. 1981.

[13]Babcock, C. D., "Shell Stability," *Journal of Applied Mechanics, Proceedings of the ASME*, Vol. 50, 1983, pp. 935–940.

[14]Kapania, R. K. and Yang, T. Y., "Formulation of an Imperfect Quadrilateral Doubly Curved Shell for Postbuckling Analysis," *AIAA Journal*, Vol. 24, 1986, pp. 310–311.

[15]McNamara, J. F. and Marcal, P. V., "Incremental Stiffness Method for Finite Element Analysis of the Nonlinear Dynamic Problem," *International Mechanics*, Urbana, IL, Sept. 1971, pp. III-4-1—III-4-35.

[16]Kao, R. and Perrone, N., "Dynamic Buckling of Axisymmetric Spherical Caps with Initial Imperfections," *Computers and Structures*, Vol. 9, 1978, pp. 463–473.

[17]Lockhart, D. F., "Post-buckling Dynamic Behavior of Periodically Supported Imperfect Shells," *International Journal of Nonlinear Mechanics*, Vol. 17, 1982, pp. 165–174.

[18]Holzer, S., "Dynamic Stability of Elastic Imperfection-Sensitive Shells," *The Shock and Vibration Digest*, Vol. 8, No. 4, 1976, pp. 3–10.

[19]Jones, N., "Dynamic Elastic and Inelastic Buckling of Shells," *Developments in Thin-Walled Structures—2*, edited by J. Rhodes and A. C. Walker, Elsevier, England, 1984, pp. 49–91.

[20]Argyris, J. H. and Scharpf, D. W., "The SHEBA Family of Shell Elements for the Matrix Displacement Method," *The Aeronautical Journal of the Royal Aeronautical Society*, Vol. 72, 1968, pp. 873–883.

[21]Moore, C. J., Yang, T. Y., and Anderson, D. C., "A New 48 d.o.f. Quadrilateral Shell Element with Variable Order Polynomial and Rational B-spline Geometries with Rigid Body Modes," *International Journal for Numerical Methods in Engineering*, Vol. 20, 1984, pp. 2121–2142.

[22]Yang, T. Y. and Saigal, S., "A Curved Quadrilateral Element for Static Analysis of Shells with Geometric and Material Nonlinearities," *International Journal for Numerical Methods in Engineering*, Vol. 21, 1985, pp. 617–636.

[23]Niordson, F. I., *Introduction to Shell Theory, Solid Mechanics*, Technical University of Denmark, Lyngby, Denmark, March 1980.

[24]Koiter, W. T., "General Equations of Elastic Stability of Thin Shells," *Proceedings, Theory of Shells*, edited by D. Muster, University of Houston, Houston, TX, 1967, pp. 21–36.

[25]Bathe, K. J., Ramm, E., and Wilson, E. L., "Finite Element Formulations for Large Deformation Dynamic Analysis," *International Journal for Numerical Methods in Engineering*, Vol. 9, 1975, pp. 353–386.

[26]Zienkiewicz, O. C., *The Finite Element Method*, 3rd ed., McGraw-Hill, London, England, 1977.

[27]Hui, D. and Leissa, A. W., "Effects of Unidirectional Geometric Imperfections on Vibrations of Pressurized Shallow Spherical Shells," *International Journal of Nonlinear Mechanics*, Vol. 18, 1983, pp. 279–285.

[28]Koiter, W. T., "The Nonlinear Buckling Problem of a Complete Spherical Shell Under Uniform External Pressure," I, II, III and IV, *Proceedings*, Kon. Ned. At. Wet., B72 40–123, 1969.

[29]Kalnins, A. and Biricikoglu, V., "On the Stability Analysis of Imperfect Spherical Shells," *Journal of Applied Mechanics, Proceedings of the ASME*, Vol. 37, 1970, pp. 629–634.

[30]Hutchinson, J. W., "Imperfection-Sensitivity of Externally Pressurized Spherical Shells," *Journal of Applied Mechanics, Proceedings of the ASME*, Vol. 34, 1967, pp. 49–55.

[31]Tong, P. and Pian, T. H. H., "Postbuckling Analysis of Shells of Revolution by the Finite Element Method," *Thin Shell Structures: Theory, Experiment and Design*, edited by Y. C. Fung and E. F. Sechler, Prentice-Hall, NJ, 1974, pp. 435–442.

[32]Shiau, A. C., Roth, R. S., and Soong, T. T., "Dynamic Buckling of Conical Shells with Imperfections," *AIAA Journal*, Vol. 12, 1974, pp. 755–760.

[33]Koga, T. and Hoff, N. J., "The Axisymmetric Buckling of Initial Imperfection Complete Spherical Shells," SUDDAR 32, Stanford University, CA, May 1968.

[34]Hibbit, H. D. and Marcal, P. V., "Hybrid Finite Element Analysis with Particular Reference to Axisymmetric Structures, AIAA Paper 70-137, Jan. 1970.